LANGMUIR

pubs.acs.org/Langmuir Article

Impact of Shell Composition on Dye Uptake by Capsules of Ionic Liquid

Katelynn Edgehouse, Nicholas Starvaggi, Neil Rosenfeld, David Bergbreiter, and Emily Pentzer*

Cite This: *Langmuir* 2022, 38, 13849−13856 Read Online

ACCESS | Metrics & More | Article Recommendations | Supporting Information

ABSTRACT: Encapsulation of ionic liquids (ILs) has been shown to be an effective technique to overcome slow mass transfer rates and handling difficulties that stem from the high viscosity of bulk ILs. These systems commonly rely on diffusion of small molecules through the encapsulating material (shell), into the IL core, and thus the composition of the shell impacts uptake performance. Herein, we report the impact of polymer shell composition on the uptake of the small molecule dye methyl red from water by encapsulated IL. Capsules with core of 1-hexyl-3-methylimidazolium bis(trifluorosulfonyl)imide ([Hmim][TFSI]) were prepared by interfacial polymerization in emulsions stabilized by graphene oxide (GO) nanosheets; the use of different diamines and diisocyanates gave capsule shells with polyureas that were all aliphatic, aliphatic/aromatic, and aliphatic/polar aprotic. These capsules were then added to aqueous solutions of methyl red at different pH values, and migration of the dye into the capsules was monitored by UV−vis spectroscopy, compared to the capsule shell alone. Regardless of the polymer identity, similar extents of dye uptake were observed (>90% at pH = 2), yet capsules with shells containing polyureas with polar aprotic linkages took longer to reach completion. These studies indicate that small changes in capsule shell composition can lead to different performance in small molecule uptake, giving insight into how to tailor shell composition for specific applications, such as solvent remediation and gas uptake.

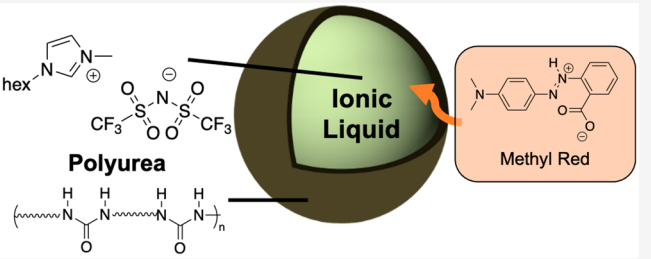

INTRODUCTION

Ionic liquids (ILs) are molten organic salts with melting points below 100 °C, with some having melting points below room temperature.[1] ILs have several favorable properties, including good ionic conductivity, good thermal and chemical stability, and negligible vapor pressures, and thus their use in extractions and separations has garnered widespread interest.[2,3] However, the high viscosities of ILs limit such applications due to slow mass transfer rates. To overcome these challenges, the accessible surface area of the IL must be increased. This is accomplished, most commonly by physical agitation (which requires additional energy input and can result in formation of undesired emulsions) or by encapsulation. Compared to bulk ILs, encapsulated ILs have improved performance in gas uptake and contaminant removal[4,5] with the additional benefit of being handled as a solid (e.g., powder).

Methods to encapsulate ILs include filling a hollow shell with the desired liquid (i.e., hard template method), the microfluidic approach, and using an emulsion as a template for interfacial polymerization (i.e., soft template method). Microfluidic techniques provide excellent control over capsule diameter and shell thickness but require monomers that are immiscible in both the droplet and the continuous phase and may not be fully viable for viscous ILs.[6] Alternatively, in the hard template method, a shell is first grown on a rigid template (such as silica particles), giving control of shell size and integrity;[7,8] then the template is removed, and the hollow capsule is backfilled with an IL. This approach was used by Moya et al. to encapsulate the IL trihexyl(tetradecyl)-phosphonium 2-cyanopyrrolide ($[P_{66614}][2\text{-CNpry}]$) in a shell of porous carbon; the capsules preserved the CO_2 uptake capabilities of the neat IL and had enhanced CO_2 adsorption rates stemming from the increased gas−IL surface contact area.[9] However, this approach required hydrofluoric acid (HF) to remove the silica template, and impregnation of the hollow shell required a cosolvent (acetone) followed by its evaporation. Alternatively, the soft templating approach is highly attractive for encapsulating ILs, as it can produce capsules with different shell compositions in a single synthetic step, including the production of capsules with cores of viscous ILs.

Our group and others have reported the use of interfacial polymerization in Pickering emulsions or those stabilized by solid polymer particles to produce capsules by the soft

Received: July 27, 2022
Revised: October 18, 2022
Published: October 31, 2022

https://doi.org/10.1021/acs.langmuir.2c02015
Langmuir 2022, 38, 13849−13856

template method.[1,10] For example, Luo et al. used an emulsion stabilized by alkylated graphene oxide (GO) nanosheets to encapsulate the IL 1-butyl-3-methylimidazolium tetrafluoroborate ([Bmim][BF_4]) in a composite shell of alkylated GO/polyurea via interfacial polymerization between a diamine and diisocyanate. Since this bulk IL had previously be used to separate phenol from hydrocarbons,[11] these capsules were used as column packing material to removal phenol from hexanes, where the IL core dictated contaminant removal, giving an eluent of pure oil.[12] This study indicates that the small molecule phenol migrated from the oil to the shell and then from the shell into the IL core. Our group also demonstrated that IL capsules have excellent performance in the capture of CO_2, with both the IL core and the shell contributing to gas uptake.[4,13,14] More recently, we prepared capsules with a core of the hydrocarbon lubricant poly(α-olefin) (PAO) (M_n = 432 Da) via the soft template method and demonstrated their use for removal of benzene, toluene, ethylbenzene, and xylene (BTEX) contaminants from water.[15] These prior proof-of-concept demonstrations illustrate that capsules with a liquid core and shell of polyurea and nanosheets can be used for rapid uptake of small molecules from water, organic solvents, or air and that the modularity of the soft template platform inspires tuning the shell and core for specific applications.

Herein, we evaluate the impact of the polymer shell identity of IL capsules on uptake of the small molecule dye methyl red from aqueous solutions at different pH (i.e., with methyl red of different charge). Since the small molecule diffuses from water to the shell to the core, we posit that the identity of the polymer and small molecule dye will impact not only whether the capsules uptake the small molecule but also the rate at which this occurs. Capsules with a core of the IL 1-hexyl-3-methylimidazolium bis(trifluorosulfonyl)imide ([Hmim][TFSI]) were prepared from an IL-in-water Pickering emulsion stabilized by GO nanosheets; the IL contained a diisocyanate, and a diamine was introduced to the continuous phase so that interfacial polymerization formed a composite shell of polyurea and nanosheets around the IL core. Three different polyurea shells were prepared: all aliphatic, aliphatic/aromatic, and aliphatic/polar aprotic. Capsules with the most hydrophilic polymer shell required a longer time for dye uptake, and control experiments using a wax core revealed that this polymer itself contributed more to dye uptake than the others. We further probed the impact of a small molecule charge on uptake into the IL. These studies showed that both bulk and encapsulated IL had a significantly higher affinity for methyl red at pH 2 (zwitterionic form) than at pH 12 (anionic) and that the capsule shell impacts the rate of dye uptake but not the final amount.

EXPERIMENTAL SECTION

Materials. 1,6-Hexanediisocyanate (HDI, 822−06−0), tolylene-2,4-diisocyanate (TDI, 84−84−9), ethylenediamine (EDA, 107−15−3), propylamine (107−10−8), methyl red (crystalline, ACS Reagent, 493−52−7), hydrochloric acid (37%, ACS reagent, 7647−01−0), sodium citrate monobasic (purum, 18996−35−5), citric acid (99%, 77−92−9), hexanes (110−54−3), and isopropanol (200−661−7) were purchased from MilliporeSigma. Mesitylene (108−67−8) was purchased from Acros Organics. *n*-Eicosane (112−95−8) was obtained from Alfa Aesar. Jeffamine EDR-148 (929−59−9) was obtained from Huntsman. Acetone-d_6 (666−52−4) was purchased from Cambridge Isotope. 1-Hexyl-3-methylimidazolium bis(trifluorosulfonyl)imide ([Hmim][TFSI], 382150−50−7) was obtained from Iolitec. Sodium hydroxide pellets (1310−73−2) were purchased from Oakwood Chemical.

Instrumentation. Emulsification was done with a BioSpec Products Inc. hand-held emulsifier (model number 985370). Centrifugation was completed with a Thermo Scientific Sorvall ST 8 centrifuge, with samples undergoing centrifugation at 4500 rpm for 10 min. A Fisherbrand CPX3800 Ultrasonic Bath 5.7 L was used for sonication along with a Fisherbrand vortex mixer for vortex mixing. A VEVOR orbital rotating shaker was used to agitate samples for dye movement experiments. Optical microscopy images were taken using an AmScope 150C-2L microscope equipped with an 18 MP USB 3.0 camera. To prepare samples for imaging, approximately 5 mg of capsules was placed on a glass slide and dispersed by adding a couple drops of water (EDA+HDI, EDA+TDI polyurea capsules) or isopropanol (JA EDR-148+HDI polyurea capsules). Fourier transform infrared spectroscopy (FTIR) used a JASCO FT/IR-4600 with a ZnSe/diamond prism with 16 scans in ATR mode. ^{1}H NMR nuclear magnetic resonance spectroscopy was carried out using a Bruker Avance NEO 400 mHz NMR spectrometer. UV−vis analysis was carried out on a Shimadzu UV-2600 UV−vis spectrophotometer, scanning wavelengths from 700 to 300 nm. Particle size analysis was completed on a Horiba Partica LA960 particle sizer. A minute quantity (<50 mg) of capsules was gently dispersed in methanol. Analysis was accomplished via dynamic light scattering, while the sample was under magnetic stirring.

Synthesis of [Hmim][TFSI] Capsules. Graphene oxide (GO) was prepared following a modified Hummer's method,[1] as previously reported.[10,12] GO was then dispersed in distilled water at a concentration of 2 mg/mL (GO stock), and 1 μL of saturated NaCl solution was added for every 1 mL of GO stock. Then, 1 mL of [Hmim][TFSI] was added to a vial, followed by 1.3 mmol of diisocyanate (see Table S1 for detailed amounts). Next, 5 mL of the GO stock solution was added to the vial, and the two liquids were emulsified with a hand-held emulsifier for three cycles of 20 s on, 15 s off. Following emulsification, 0.50 mL of water was added to dilute the emulsion. At this point, a solution of 1.7 mmol amine (Table S1) in 1.25 mL of distilled water as then added dropwise with hand swirling to the emulsion. The emulsion was then left unagitated under ambient conditions for 72 h. Then, the capsules were collected via gravity filtration, washed with distilled water, and placed in 100 mL of a solution of 7 v/v% propylamine in distilled water for 24 h to quench any remaining unreacted isocyanate functional groups. The quenched capsules were then isolated via gravity filtration and washed again with distilled water until the supernatant achieved a neutral pH. Finally, the capsules were dried under reduced pressure at 30 °C, resulting in a light brown powder.

Synthesis of *n*-Eicosane Capsules. *n*-Eicosane capsules were synthesized following a similar procedure to that of [Hmim][TFSI] capsules. Briefly, *n*-eicosane was heated to 50 °C to ensure it was in its liquid state. Then, 1 mL of *n*-eicosane was added to a vial, followed by the corresponding 1.3 mmol of diisocyanate (Table S1). The vial was then left at 50 °C until all contents were a clear liquid. Next, 5 mL of the same GO stock solution from above that had been warmed to 50 °C was added to the molten *n*-eicosane mixture. At this point, the system was kept on the 50 °C hot plate and emulsified with a hand-held emulsifier for three cycles of 20 s on and 15 s off. Then, 0.50 mL of warm water was added to the emulsion to dilute it, followed by the addition of 1.7 mmol diamine in 1.25 mL of distilled water (Table S1) dropwise with hand swirling. The resulting emulsion was then left to sit at room temperature for 72 h, resulting in solid particles of *n*-eicosane with a GO/polyurea shell. The capsules were isolated via gravity filtration, washed with distilled water, and then added to 100 mL of a 7 v/v% solution of propylamine in distilled water for 24 h to quench any unreacted isocyanate functional groups. The quenched capsules were then isolated via gravity filtration, washed with distilled water until the supernatant achieved a neutral pH, and dried under reduced pressure at ambient temperature, resulting in a light brown powder.

Determination of [Hmim][TFSI] Weight Percent in Capsules via ^{1}H NMR. Following a previously reported procedure,[2]

https://doi.org/10.1021/acs.langmuir.2c02015
Langmuir 2022, 38, 13849−13856

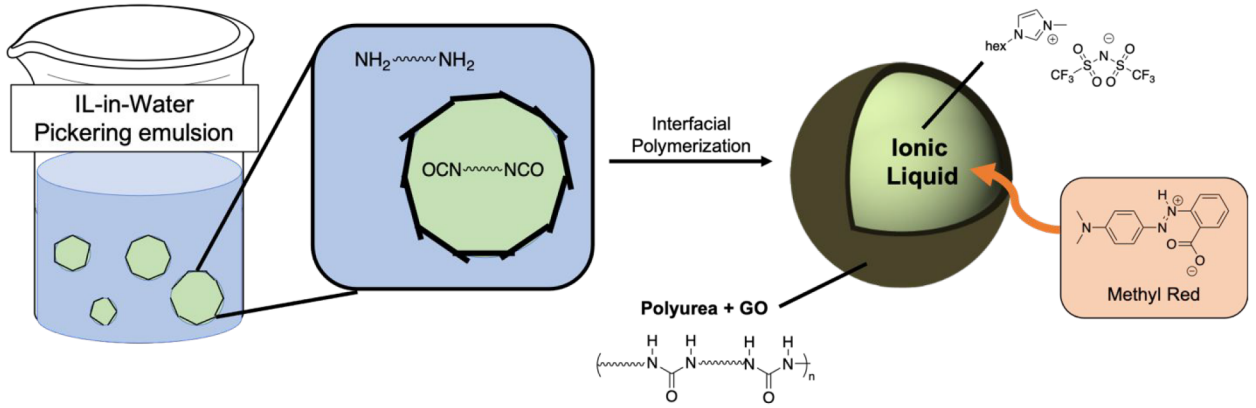

Figure 1. Overview of this work: synthesis of capsules with core of [Hmim][TFSI] and shell of polyurea and graphene oxide nanosheets via interfacial polymerization and migration of methyl red into capsule.

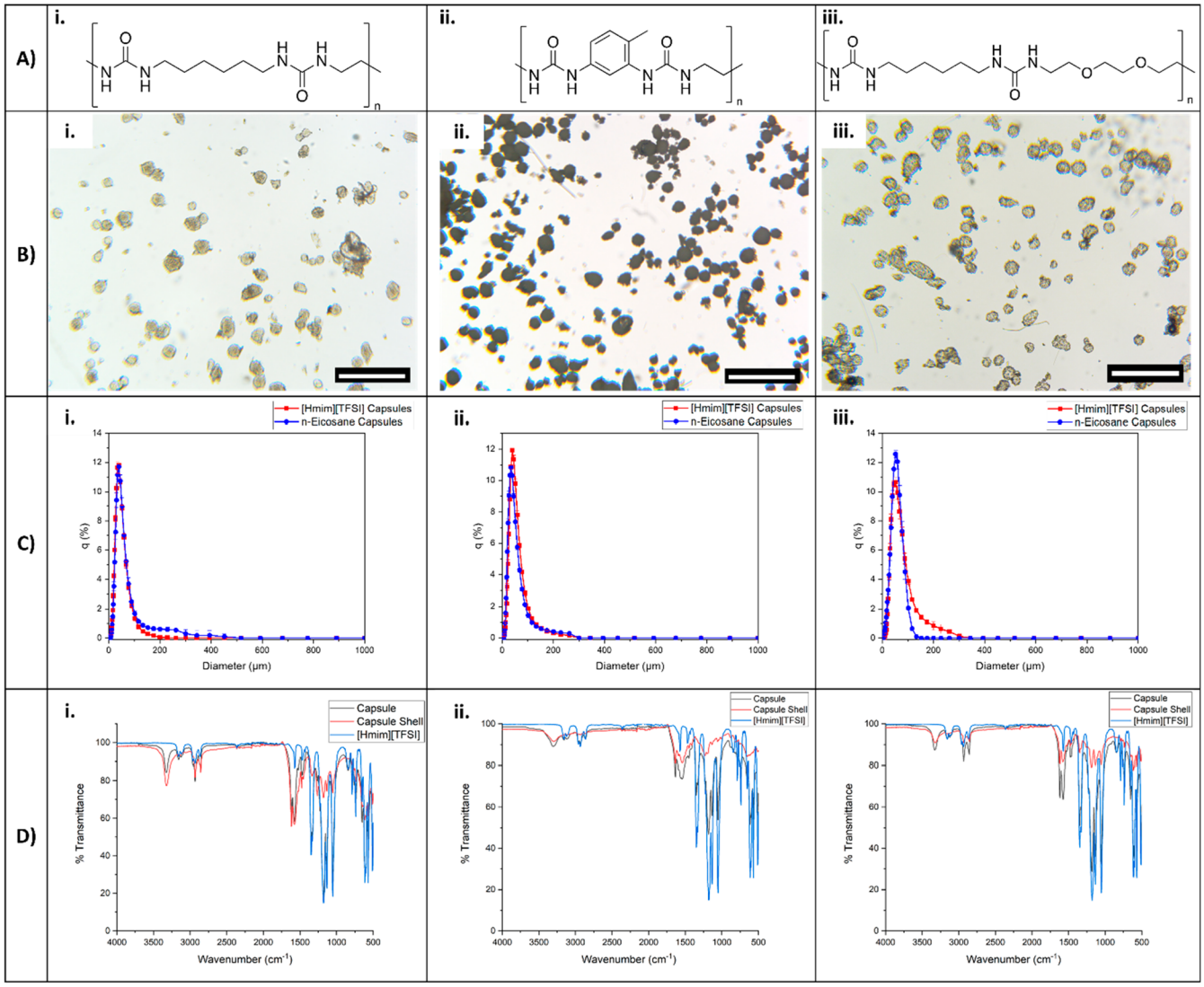

Figure 2. Chemical structure of the polyurea shells: (A) (i) EDA+HDI (all aliphatic), (ii) EDA+TDI (aliphatic/aromatic), and (iii) JA EDR-1478+HDI (aliphatic/polar aprotic); (B) optical microscopy images of [Hmim][TFSI] capsules with shells corresponding to the polyureas in A; (C) particle size analysis data of each capsule system; and (D) FTIR spectra of the capsule, capsule shell, and neat [Hmim][TFSI]. Scale bars are 200 μm.

approximately 20 mg of [Hmim][TFSI] capsules was weighed out and placed into a vial containing 0.039 M mesitylene (internal standard) in acetone-d_6. The mixture was then sonicated for 30 min to release all [Hmim][TFSI] from the capsule core. Next, the solution

https://doi.org/10.1021/acs.langmuir.2c02015
Langmuir 2022, 38, 13849−13856

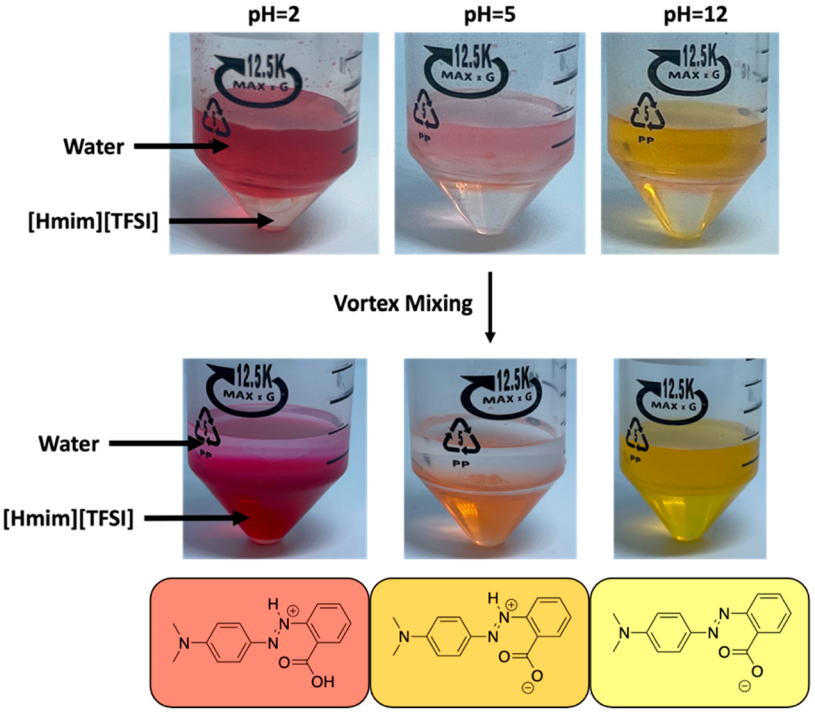

Figure 3. Aqueous/IL biphasic systems showing the movement of methyl red from aqueous solutions of different pH values to neat [Hmim][TFSI]. The biphasic solution was vortex mixed then centrifuged to expedite phase separation. Boxes at the bottom illustrate the impact of aqueous pH on methyl red color and charge: +1 and red in acidic conditions (pH = 2), zwitterionic and orange at intermediate pH values (pH = 5), and anionic and yellow in basic conditions (pH = 12).

was passed through a poly(tetrafluoroethylene) (PTFE) syringe filter (0.2 μm pore size) to remove the broken shell material and then placed in an NMR tube for ^{1}H NMR analysis. Weight percent encapsulated [Hmim][TFSI] could then be determined by comparing the relative integration of the methyl peak from mesitylene (2.20 ppm) to the methyl peak of the [Hmim] cation (4.06 ppm) (Figure S1). This was repeated 3 times, using samples from different capsule batches.

Determination of *n*-Eicosane Weight Percent of Capsules via Mass Difference. 100 mg of *n*-eicosane capsules was added to 10 mL of hexanes. Then, the solution was sonicated for 30 min to isolate the *n*-eicosane from the capsule core. The solution was then passed through a PTFE syringe filter (0.2 μm pore size) to remove the broken shell material. The *n*-eicosane was then separated from the hexanes by subjecting the solution to rotary evaporation. After rotary evaporation, *n*-eicosane would remain in the vessel as a white solid. The mass of this white solid was determined and then compared to the initial capsule mass to determine weight percent.

Monitoring Methyl Red Movement into [Hmim][TFSI] Capsules. First, solutions of 0.2 mg/mL methyl red were prepared in 0.01 M HCl (pH = 2), 0.01 M NaOH (pH = 13), and a 0.1 M citrate buffer at pH = 5. The citrate buffer was prepared by dissolving 21 g sodium citrate monobasic and 0.2 g citric acid in 1 L of water. 0.01 M HCl and 0.01 M NaOH were added dropwise until a pH of 5 was confirmed via litmus paper. The solutions of methyl red were sonicated until all methyl red had dissolved. For a given experiment, 100 mg of [Hmim][TFSI] capsules were added to a 50 mL centrifuge tube, followed by 10 mL of methyl red solution. The mixtures were then placed on an orbital shaker and agitated at 150 rpm for 2 h, with intermittent sampling of the aqueous phase done for UV−vis analysis to monitor the percent of methyl red remaining in the aqueous phase. For acidic methyl red solutions, 0.50 mL of sample was added to 9.5 mL of 0.01 M HCl. For basic methyl red solutions, 0.50 mL of sample was added to 19.5 mL of 0.01 M NaOH. For buffered methyl red solutions, 0.50 mL of sample was added to 4.5 mL of 0.01 M HCl. Different volumes were required to ensure that measured absorbances fell within the calibration curve. All buffer samples were acidified prior to UV−vis analysis, as both the basic and acidic forms of methyl red are present, which otherwise causes one broad plateau in the resultant UV−vis spectrum instead of a sharp peak. Both acidic and basic calibration curves were made, with the peak at 432 nm used for basic samples and the peak at 525 nm used for acidic samples (Figures S2 and S3). All experiments were done in triplicate to ensure reproducibility.

To determine how methyl red interacts with the capsule shell material, capsules of *n*-eicosane and [Hmim][TFSI] were allowed to saturate with methyl red, and the corresponding decrease in aqueous phase concentration measured. This was done by adding 10 mg of either *n*-eicosane or [Hmim][TFSI] capsules to 10 mL of aqueous methyl red (acidic and buffered). These systems were then agitated on an orbital shaker at 150 rpm for 24 h. Samples of the continuous phase were collected for analysis, following the pH dependent sampling procedures outlined above.

RESULTS AND DISCUSSION

[Hmim][TFSI]-in-water Pickering emulsions stabilized by GO nanosheets were used as a template to encapsulate [Hmim][TFSI] in a GO/polyurea shell via interfacial polymerization (Figure 1).[12,13] As a control, capsules with a core of solid *n*-eicosane wax were also prepared using interfacial polymerization via a GO stabilized molten wax-in-water Pickering emulsion template, followed by cooling; these particles with a wax core enabled characterization of the uptake due to the polymer shell alone (i.e., not the IL). All capsules were characterized via optical microscopy and Fourier transform infrared (FTIR) spectroscopy, and particle size distributions were determined via laser diffraction studies. The weight percent of [Hmim][TFSI] in the capsules was determined via quantitative proton nuclear magnetic resonance (^{1}H NMR) spectroscopy following extraction with acetone-d_6 containing mesitylene as an internal standard; composition of the *n*-

https://doi.org/10.1021/acs.langmuir.2c02015
Langmuir 2022, 38, 13849−13856

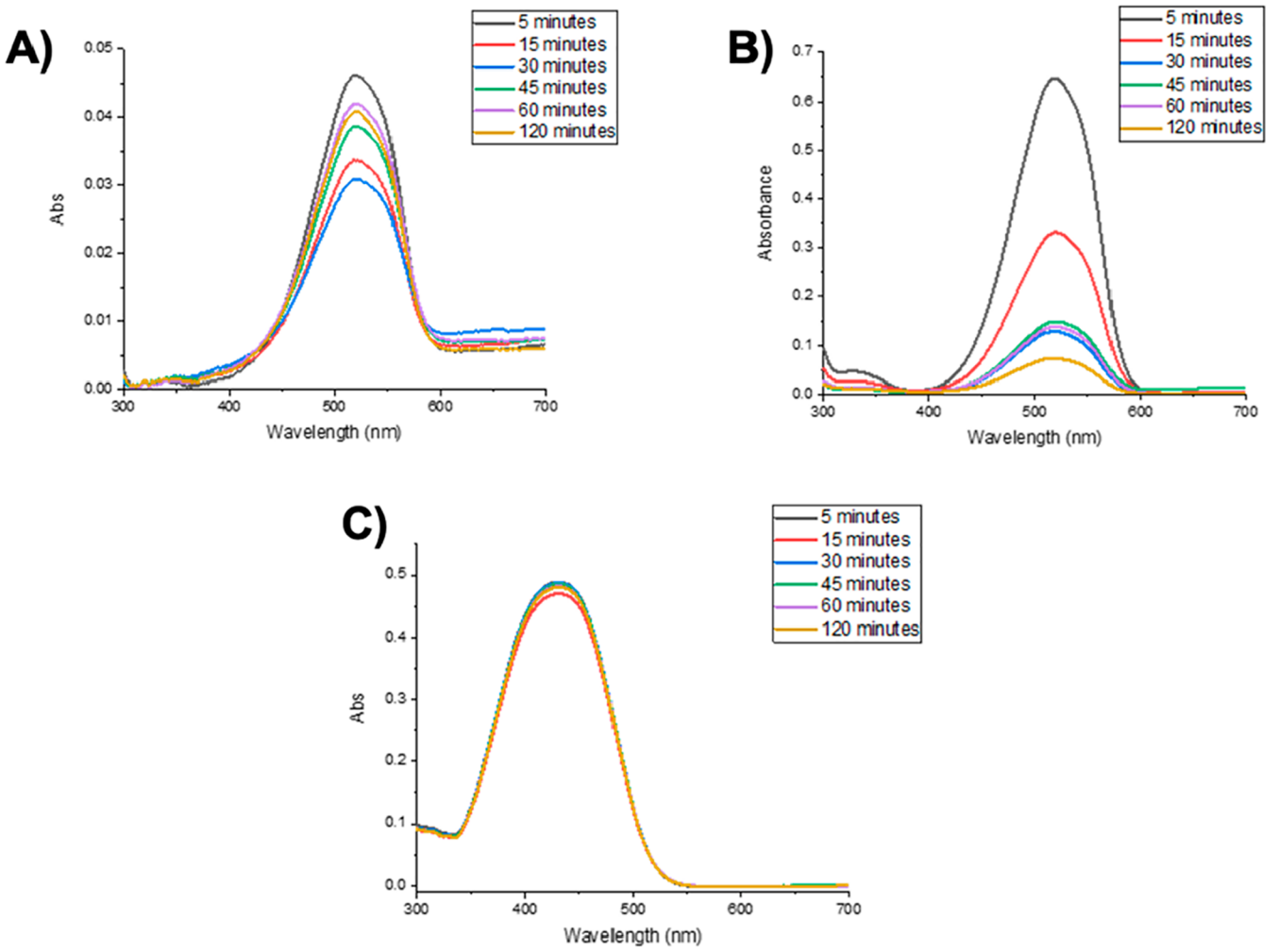

Figure 4. UV−vis spectra of the aqueous solution of methyl red after swirling with capsules of [Hmim][TFSI] with shells containing EDA + HDI at (A) pH = 2; (B) pH = 5; and (C) pH = 12. The difference in the range of values of the *y*-axis is due to differences in solubility of the dye.

eicosane capsules was determined by extracting the solid wax core, removing solvent, and weighing the extracted *n*-eicosane (see Supporting Information for details).

Three different monomer systems were investigated to prepare capsule shells: ethylenediamine (EDA) and 1,6-hexanediisocyanate (HDI), EDA and tolylene-2,4-diisocyanate (TDI), and Jeffamine EDR-148 (JA EDR-148) and HDI (Table S1). These monomer systems were chosen as they provide varied polyurea structure: EDA+HDI produces an aliphatic polyurea, EDA+TDI an aliphatic/aromatic polyurea, and JA EDR-148+HDI a more hydrophilic aliphatic/polar aprotic polyurea (Figure 2A). All monomer systems produced discrete, semispherical capsules with average diameters of ∼50 μm (Figure 2B and C; Table S2); the slightly irregular shape of the capsule is attributed to the method used for fabrication (e.g., interfacial polymerization) and solvent evaporation during drying. FTIR analysis confirmed the successful reaction between isocyanate and amine groups, as indicated by a lack of stretching frequency from 2275 to 2250 cm^{-1}, which would indicate unreacted isocyanate groups. Further, stretches at 3400 and 1600 cm^{-1} indicate the presence of N−H and C═O bonds of the polyurea, respectively (Figure 2D). All [Hmim][TFSI] capsules had similar weight percentages of [Hmim][TFSI] (∼70 wt %, Table S2, Figure S1), indicating that these capsules are structurally similar. The *n*-eicosane capsules showed similar diameters and weight percentages of core material in comparison to IL capsules (Table S2).

Methyl red dye was chosen as the small molecule to monitor moving into the capsules, because ILs have previously been used to isolate azo dyes from aqueous solutions in bulk extractions.[16,17] Further, the charge of methyl red depends on pH of the aqueous solution (Figure 3) and the distinctive absorption profile of the small molecule allows for monitoring using UV−vis spectroscopy. At pH values below 4.4, methyl red is cationic with a net +1 charge and red in color (protonated azo nitrogen and $-CO_2H$ group). At high pH values, methyl red is yellow and is anionic with a net −1 charge (neutral azo group and $-CO_2^-$ group).[18,19] At pH values between 4.4 and 6.2, the dominant species is zwitterionic and the solution is orange (protonated azo nitrogen and a $-CO_2^-$ group). Thus, to investigate the impact of pH on methyl red movement into the IL capsules, a known amount of methyl red was dissolved in aqueous HCl (pH = 2, red), aqueous citrate buffer (pH = 5, orange), or aqueous NaOH (pH = 12, yellow). Calibration curves were then prepared using UV−vis absorption spectroscopy (λ_{max} = 525 nm for pH 2; λ_{max} = 432 nm for pH 12, see Figure S2 and Figure S3 for calibration curves). Notably, a reliable calibration curve could not be prepared for the buffered solutions, so samples were acidified

https://doi.org/10.1021/acs.langmuir.2c02015
Langmuir 2022, 38, 13849−13856

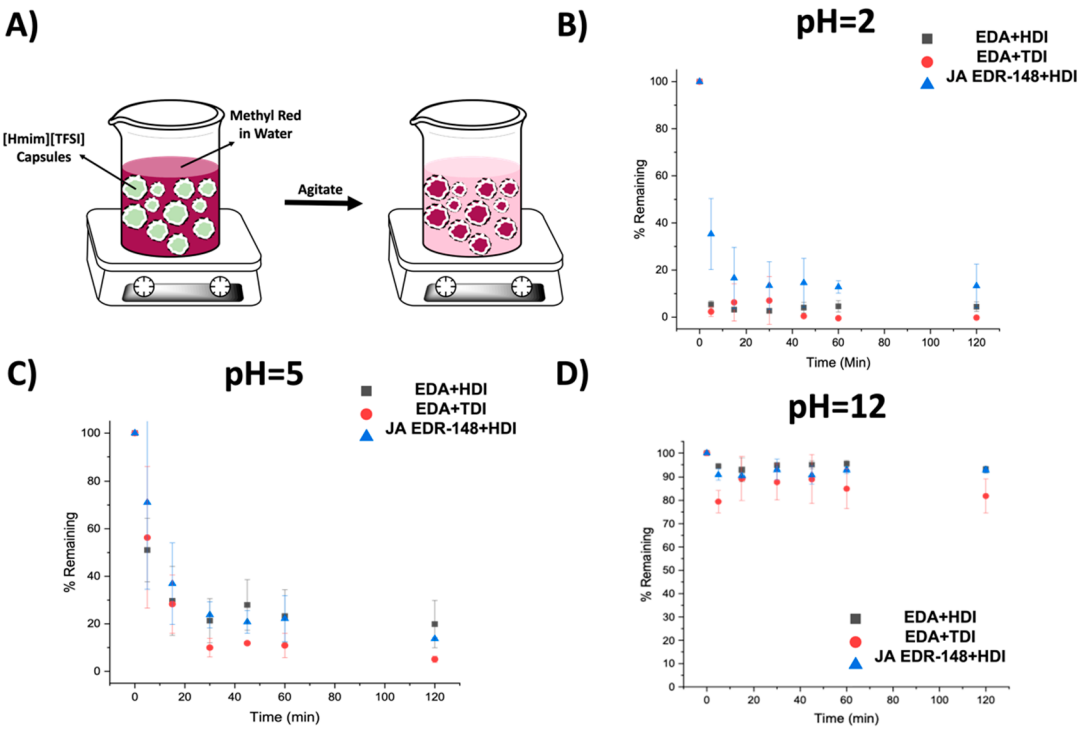

Figure 5. (A) Schematic of experimental set up for monitoring dye movement, and percent of methyl red remaining in the continuous aqueous phase over time after agitation in with [Hmim][TFSI] capsules at (B) pH = 2; (C) pH = 5; and (D) pH = 12.

before characterization by UV−vis and concentrations determined using the calibration curve at pH = 2.

To ensure that methyl red was a suitable dye to study the permeability of various GO/polyurea capsule shells, first the migration of methyl red from water to bulk [Hmim][TFSI] was evaluated in a biphasic mixture. This was completed by adding aqueous methyl red to nonencapsulated [Hmim]-[TFSI] and mixing by vortex for 1 min, then centrifuging to expedite phase separation (Figure 3); the concentration of methyl red in the aqueous phase was then determined by UV−vis. When the aqueous phase was acidic, the red color of the aqueous phase diminished and the [Hmim][TFSI] phase became transparent and dark red, suggesting that the dye moved from the aqueous to the IL phase. UV−vis analysis of the aqueous phase confirmed that <1% of the methyl red remained in the aqueous phase after mixing and phase separation (Figure S4A). Conversely, when the aqueous phase was basic, only a slight color change was observed for the [Hmim][TFSI] phase and the aqueous phase remained yellow; UV−vis spectroscopic analysis showed that 82% of methyl red remained in the aqueous phase (Figure S4B). When the aqueous phase had an intermediate pH of 5 (buffered), the [Hmim][TFSI] phase took on an orange color and the aqueous phase largely lost its color, suggesting that some methyl red moves into the [Hmim][TFSI]. These data support that the affinity of methyl red for [Hmim][TFSI] is dependent on the pH of the aqueous phase with most of the dye transferring from the aqueous phase to IL phase at pH = 2 but not at pH = 12.

Next, dye movement of methyl red into encapsulated [Hmim][TFSI] from aqueous solutions at different pH was evaluated for the EDA+HDI capsules. The capsules were suspended in 10 mL of aqueous methyl red solutions at a given pH, then the vial was agitated on an orbital shaker, and the concentration of methyl red in the aqueous phase was monitored via UV−vis spectroscopy at regular intervals over 2 h. The UV−vis spectra for each sample are shown in Figures 4. In line with the bulk, biphasic experiments discussed above, the capsules were able to readily uptake methyl red from the acidic solution, and after 15 min, 8% of the dye remained in the water (with no significant change after 2 h of stirring, see Figure 4A and B). In contrast, little methyl red was uptaken by the capsules from basic solution, and 94% of the dye remained in the water after 2 h of stirring (see Figure 4C and Figure 5D). For the buffered aqueous solution, 15% of the dye remained in the water after stirring with the capsules (Figure 4B and Figure 5C). These results are consistent with what was observed for the bulk water/IL systems.

Figure 5 shows the precent dye remaining in the aqueous solution after treatment with the capsules over time based on the pH of the aqueous phase and polymer composition. Whereas all polymer shells show similar trends, the identity of the polyurea does impact the kinetics of uptake to a certain extent (see Figures S5−S7 for UV−vis spectra). All IL capsules eventually show >90% dye sequestration from acidic aqueous solution after 2 h, suggesting that favorable van der Waals interactions between the polymer and both the zwitterionic and anionic dye facilitate movement of the dye from water to the shell and from the shell to the IL. However, capsules with the JA EDR-148+HDI polyurea (aliphatic/polar aprotic) take twice as long to reach dye saturation (i.e., 30 min as compared to 15 min for the other two systems). As the defining difference between JA EDR-148+HDI polyurea and the others is the polar aprotic ether linkages (e.g., diethylene glycol vs hexyl), these data suggest that small changes in polarity of the polymer may slow transfer of the dye from the shell to the IL.

To confirm that methyl red was moving into the [Hmim][TFSI] core of the capsules and that uptake was not

https://doi.org/10.1021/acs.langmuir.2c02015
Langmuir 2022, 38, 13849−13856

solely attributed to the polymer shell, capsules with core of IL and solid *n*-eicosane were agitated overnight in solutions of methyl red at pH 2 and pH 5, with changes of methyl red concentration in the aqueous phase again monitored via UV−vis spectroscopy. A decrease in concentration was observed for the *n*-eicosane capsules, thereby indicating that methyl red adsorbs to the GO/polyurea shell; however, capsules with a core of [Hmim][TFSI] removed more methyl red at both pH values (Tables S3 and S4, Figures S8−S9), highlighting the potential synergistic performance of the shell and core. For example, at pH 2, [Hmim][TFSI] capsules with EDA+HDI shell show almost complete uptake of methyl red, whereas *n*-eicosane capsules only achieve partial dye removal (2.5% and 49% dye remaining, respectively). Similar results are seen at pH 5 as well: *n*-eicosane capsules show 51% dye remaining, whereas [Hmim][TFSI] capsules show only 16% dye remaining (Tables S3 and S4). Further, the polymer identity directly impacted how much dye the capsules with solid wax core could uptake; at pH 2 all polymer shells led to ∼50% dye uptake, whereas at pH 5 the EDA+HDI and EDA+TDI capsules showed ∼50% dye uptake whereas the JA EDR-148+HDI capsules showed 75% dye uptake. Taken together, these data demonstrate that although both shell and core material can contribute to dye uptake, the core IL can indeed be accessed.

CONCLUSIONS

In summary, capsules of [Hmim][TFSI] with composite shells of GO/polyurea were prepared and used to monitor the movement of a small molecule (methyl red) across the shell into the core IL, and the impact of chemical structure of both the dye and the polymer was examined. The capsules were prepared by the soft template method and characterized by optical microscopy, laser diffraction, and FTIR spectroscopy. For all capsules and the bulk biphasic systems, significantly more methyl red migrated to the IL phase from an acidic or buffered aqueous solution (pH = 2 and pH = 5) compared to basic solution (pH = 12). Across the three polyurea shells evaluated, all reached similar levels of dye migration into the IL core (>90% at pH 2), with the aliphatic/polar aprotic polyurea taking longer than the all aliphatic and aliphatic/aromatic polyureas. Using capsules with the same shells but solid wax cores, we demonstrate that dye uptake is attributed to the IL core and not the polymer shell, which together form a complementary system. A number of factors impact migration of small molecules into and out of capsules (polymer chemistry, thermal properties, etc.), and thus tuning the capsule composition offers exciting opportunities to target properties for specific applications, including (but not limited to) contaminant remediation, gas adsorption, and electrochemical device fabrication.

ASSOCIATED CONTENT

Supporting Information

The Supporting Information is available free of charge at https://pubs.acs.org/doi/10.1021/acs.langmuir.2c02015.

UV−vis data, size distribution, and composition of capsules (PDF)

AUTHOR INFORMATION

Corresponding Author

Emily Pentzer − *Department of Chemistry and Department of Materials Science and Engineering, Texas A&M University, College Station, Texas 77843, United States;* orcid.org/0000-0001-6187-6135; Email: emilypentzer@tamu.edu

Authors

Katelynn Edgehouse − *Department of Chemistry, Texas A&M University, College Station, Texas 77843, United States;* orcid.org/0000-0003-0910-8723

Nicholas Starvaggi − *Department of Chemistry, Texas A&M University, College Station, Texas 77843, United States;* orcid.org/0000-0002-0085-7886

Neil Rosenfeld − *Department of Chemistry, Texas A&M University, College Station, Texas 77843, United States*

David Bergbreiter − *Department of Chemistry, Texas A&M University, College Station, Texas 77843, United States;* orcid.org/0000-0002-1657-0003

Complete contact information is available at: https://pubs.acs.org/10.1021/acs.langmuir.2c02015

Notes

The authors declare no competing financial interest.

ACKNOWLEDGMENTS

This work is financially supported by a grant from the National Science Foundation DMR #2103182.

REFERENCES

(1) Luo, Q.; Pentzer, E. Encapsulation of Ionic Liquids for Tailored Applications. *ACS Appl. Mater. Interfaces* **2020**, *12* (5), 5169−5176.

(2) Ahrenberg, M.; Beck, M.; Neise, C.; Keßler, O.; Kragl, U.; Verevkin, S. P.; Schick, C. Vapor Pressure of Ionic Liquids at Low Temperatures from AC-Chip-Calorimetry. *Phys. Chem. Chem. Phys.* **2016**, *18* (31), 21381−21390.

(3) Maton, C.; De Vos, N.; Stevens, C. V. Ionic Liquid Thermal Stabilities: Decomposition Mechanisms and Analysis Tools. *Chem. Soc. Rev.* **2013**, *42* (13), 5963.

(4) Lee, Y.-Y.; Edgehouse, K.; Klemm, A.; Mao, H.; Pentzer, E.; Gurkan, B. Capsules of Reactive Ionic Liquids for Selective Capture of Carbon Dioxide at Low Concentrations. *ACS Appl. Mater. Interfaces* **2020**, *12* (16), 19184−19193.

(5) Elizarova, I. S.; Luckham, P. F. Layer-by-Layer Encapsulated Nano-Emulsion of Ionic Liquid Loaded with Functional Material for Extraction of Cd^{2+}ions from Aqueous Solutions. *J. Colloid Interface Sci.* **2017**, *491*, 286−293.

(6) Li, J.; Lindley-Start, J.; Porch, A.; Barrow, D. Continuous and Scalable Polymer Capsule Processing for Inertial Fusion Energy Target Shell Fabrication Using Droplet Microfluidics. *Sci. Rep.* **2017**, *7* (1), 1−10.

(7) Zhang, Y.; Hsu, B. Y. W.; Ren, C.; Li, X.; Wang, J. Silica-Based Nanocapsules: Synthesis, Structure Control and Biomedical Applications. *Chem. Soc. Rev.* **2015**, *44* (1), 315−335.

(8) Chen, Y.; Chen, H.-R.; Shi, J.-L. Construction of Homogenous/Heterogeneous Hollow Mesoporous Silica Nanostructures By. *Acc. Chem. Res.* **2014**, *47* (1), 125−137.

(9) Moya, C.; Alonso-Morales, N.; De Riva, J.; Morales-Collazo, O.; Brennecke, J. F.; Palomar, J. Encapsulation of Ionic Liquids with an Aprotic Heterocyclic Anion (AHA-IL) for CO_2 Capture: Preserving the Favorable Thermodynamics and Enhancing the Kinetics of Absorption. *J. Phys. Chem. B* **2018**, *122* (9), 2616−2626.

(10) Luo, Q.; Wang, Y.; Yoo, E.; Wei, P.; Pentzer, E. Ionic Liquid-Containing Pickering Emulsions Stabilized by Graphene Oxide-Based Surfactants. *Langmuir* **2018**, *34* (34), 10114−10122.

(11) Hou, Y.; Ren, Y.; Peng, W.; Ren, S.; Wu, W. Separation of Phenols from Oil Using Imidazolium-Based Ionic Liquids. *Ind. Eng. Chem. Res.* **2013**, *52* (50), 18071−18075.
(12) Luo, Q.; Wang, Y.; Chen, Z.; Wei, P.; Yoo, E.; Pentzer, E. Pickering Emulsion-Templated Encapsulation of Ionic Liquids for Contaminant Removal. *ACS Appl. Mater. Interfaces* **2019**, *11* (9), 9612−9120.
(13) Huang, Q.; Luo, Q.; Wang, Y.; Pentzer, E.; Gurkan, B. Hybrid Ionic Liquid Capsules for Rapid CO2 Capture. *Ind. Eng. Chem. Res.* **2019**, *58*, 10503.
(14) Gaur, S. S.; Edgehouse, K. J.; Klemm, A.; Wei, P.; Gurkan, B.; Pentzer, E. B. Capsules with Polyurea Shells and Ionic Liquid Cores for CO2 Capture. *J. Polym. Sci.* **2021**, *59* (23), 2980−2989.
(15) Edgehouse, K. J.; Rosenfeld, N.; Bergbreiter, D. E.; Pentzer, E. B. Capsules of the Poly(α-Olefin) PAO_{432} for Removal of BTEX Contaminants from Water. *Ind. Eng. Chem. Res.* **2021**, *60* (40), 14455−14463.
(16) Vijayaraghavan, R.; Vedaraman, N.; Surianarayanan, M.; MacFarlane, D. R. Extraction and Recovery of Azo Dyes into an Ionic Liquid. *Talanta* **2006**, *69* (5), 1059−1062.
(17) Pei, Y. C.; Wang, J. J.; Xuan, X. P.; Fan, J.; Fan, M. Factors Affecting Ionic Liquids Based Removal of Anionic Dyes from Water. *Environ. Sci. Technol.* **2007**, *41* (14), 5090−5095.
(18) Tobey, S. W. The Acid Dissociation Constant of Methyl Red. A Spectrophotometric Measurement. *J. Chem. Educ.* **1958**, *35* (10), 514.
(19) Srour, R. K.; McDonald, L. M. Determination of the Acidity Constants of Methyl Red and Phenol Red Indicators in Binary Methanol− and Ethanol−Water Mixtures. *J. Chem. Eng. Data* **2008**, *53* (1), 116−127.

https://doi.org/10.1021/acs.langmuir.2c02015
Langmuir 2022, 38, 13849−13856